J|A|C|S

A R T I C L E S

Molecular Packing of Lysozyme, Fibrinogen, and Bovine Serum Albumin on Hydrophilic and Hydrophobic Surfaces Studied by Infrared−Visible Sum Frequency Generation and Fluorescence Microscopy

Joonyeong Kim and Gabor A. Somorjai*

Contribution from the Department of Chemistry, University of California, Berkeley, California 94720, and Materials Sciences Division, Lawrence Berkeley National Laboratory, Berkeley, California 94720

Received October 17, 2002 ; E-mail: somorjai@socrates.berkeley.edu

Abstract: Infrared−visible sum frequency generation (SFG) vibrational spectroscopy, in combination with fluorescence microscopy, was employed to investigate the surface structure of lysozyme, fibrinogen, and bovine serum albumin (BSA) adsorbed on hydrophilic silica and hydrophobic polystyrene as a function of protein concentration. Fluorescence microscopy shows that the relative amounts of protein adsorbed on hydrophilic and hydrophobic surfaces increase in proportion with the concentration of protein solutions. For a given bulk protein concentration, a larger amount of protein is adsorbed on hydrophobic polystyrene surfaces compared to hydrophilic silica surfaces. While lysozyme molecules adsorbed on silica surfaces yield relatively similar SFG spectra, regardless of the surface concentration, SFG spectra of fibrinogen and BSA adsorbed on silica surfaces exhibit concentration-dependent signal intensities and peak shapes. Quantitative SFG data analysis reveals that methyl groups in lysozyme adsorbed on hydrophilic surfaces show a concentration-independent orientation. However, methyl groups in BSA and fibrinogen become less tilted with respect to the surface normal with increasing protein concentration at the surface. On hydrophobic polystyrene surfaces, all proteins yield similar SFG spectra, which are different from those on hydrophilic surfaces. Although more protein molecules are present on hydrophobic surfaces, lower SFG signal intensity is observed, indicating that methyl groups in adsorbed proteins are more randomly oriented as compared to those on hydrophilic surfaces. SFG data also shows that the orientation and ordering of phenyl rings in the polystyrene surface is affected by protein adsorption, depending on the amount and type of proteins.

Introduction

The adsorption of proteins from solution onto solid surfaces has attracted much attention due to its scientific importance and application in many areas.[1-3] In the medical and food processing industries, for example, it is usually required to remove adsorbed proteins since even a small amount of deposited protein may give rise to the subsequent adsorption of fibrous proteins, leading to adverse biological consequences.[4-6] On the other hand, controlled immobilization of proteins is crucial in the field of biotechnology, where well-ordered protein layers may lead to a new generation of reactor beds for catalysis, biosensors, and disease diagnostics.[7-9]

Previous studies with various analytical tools have produced a vast amount of information regarding protein adsorption.[1,2,10-23] These results have consistently shown that nonspecific protein adsorption is a complex phenomenon involving a series of dynamic steps from initial contact at the interface to the final

* To whom correspondence should be addressed: telephone 510-642-4053; fax 510-643-9668.

(1) *Proteins at Interfaces II: Fundamentals and Applications*; Horbett, T. A.; Brash, J. L., Eds.; American Chemical Society: Washington, DC, 1995.
(2) *Proteins at Interfaces: Physicochemical and Biochemical Studies*; Brash, J. L.; Horbett, T. A., Eds.; American Chemical Society: Washington, DC, 1987.
(3) Andrade, J. D.; Hlady, V. *Adv. Polym. Sci.* **1986**, *79*, 1−63.
(4) Sandu, C.; Singh, R. K. *Food Technol.* **1991**, *45*, 84−91.
(5) Hubbell, J. A. *Bio-Technol.* **1995**, *13*, 565−576.
(6) Ishihara, K.; Oshida, H.; Endo, Y.; Ueda, T.; Watanabe, A.; Nakabayashi, N. *J. Biomed. Mater. Res.* **1992**, *26*, 1543−1552.
(7) Rechnitz, G. A. *Chem. Engin. News* **1988**, *66*, 24−36.
(8) Martin, B. D.; Gaber, B. P.; Patterson, C. H.; Turner, D. C. *Langmuir* **1998**, *14*, 3971−3975.
(9) Inglis, W.; Sanders, G. H.; Williamsm., P. M.; Davies, M. C.; Roberts, C. J.; Tendler, S. J. B. *Langmuir* **2001**, *17*, 7402−7405.
(10) Castner, D. G.; Ratner, B. D. *Surf. Sci.* **2002**, *500*, 28−60.
(11) Wertz, C. F.; Santore, M. M. *Langmuir* **2002**, *18*, 706−715.
(12) Norde, W.; Favier, J. P. *Colloids Surf.* **1992**, *64*, 87−93.
(13) Norde, W.; Giacomelli, C. E. *Macromol. Symp.* **1999**, *145*, 125−136.
(14) Lu, J. R.; Su, T. J.; Thirtle, P. N.; Thomas, R. K.; Rennie, A. R.; Cubitt, R. *J. Colloid Interface Sci.* **1998**, *206*, 212−223.
(15) Su, T. J.; Lu, J. R.; Thomas, R. K.; Cui, Z. F.; Penfold, J. *J. Colloid Interface Sci.* **1998**, *203*, 419−429.
(16) Su, T. J.; Lu, J. R.; Thomas, R. K.; Cui, Z. F.; Penfold, J. *Langmuir* **1998**, *14*, 438−445.
(17) Sigal, G. B.; Mrksich, M.; Whitesides, G. M. *J. Am. Chem. Soc.* **1998**, *120*, 3464−3473.
(18) O'Sullivan, C. K.; Guilbault, G. G. *Biosens. Bioelec.* **1999**, *14*, 663−670.
(19) Cuppett, C. M.; Doneski, L. J.; Wirth, M. J. *Langmuir* **2000**, *16*, 7279−7284.
(20) Ortega-Vinuesa, J. L.; Tengvall, P.; Lundström, I. *Thin Solid Films* **1998**, *324*, 257−273.
(21) Kim, J.; Cremer, P. S. *ChemPhysChem* **2001**, *2*, 543−546.
(22) Kim, G.; Gurau, M.; Kim, J.; Cremer, P. S. *Langmuir* **2002**, *18*, 2807−2811.
(23) Salafsky, J. S.; Eisenthal, K. B. *J. Phys. Chem. B* **2000**, *104*, 7752−7755.

structural rearrangements on the solid substrate. The choice of solid substrate and physiological adsorption conditions (e.g., temperature, pH, and the concentrations of bulk protein solutions) is known to significantly affect the overall adsorption kinetics, the amount of adsorbed proteins, and the degree of denaturation.[1,2,13,24] The interactions between proteins and underlying solid substrates generally dictate the adsorption affinity as well as the structure of adsorbed proteins via denaturation, leading some amino acid residues to adopt a preferred orientation.

The spatial orientation of amino acid residues in adsorbed proteins on solid substrates plays an important role in subsequent biological events such as replacement, coagulation, and formation of an adsorption-resisting layer against other approaching proteins and cells.[1,2] This is especially important in biofouling and biocompatibility applications since the coagulation of proteins followed by cell adhesion is the first step in bacterial growth, contamination, and implant rejection. Studies of surface structure, such as amino acid orientation in adsorbed proteins, helps us understand and predict complex adsorption behavior, with the ultimate goal of designing surfaces that either prevent protein adsorption or form highly oriented protein layers.

For the past decade, infrared−visible sum frequency generation (SFG) vibrational spectroscopy has been used to extract information on surface structures from small molecules such as water, acetonitrile, and carbon monoxide to large molecules such as self-assembled monolayers, polymers, and proteins at various interfaces.[21,22,25−40] Fluorescence microscopy has yielded information regarding the relative amounts of adsorbed proteins on various surfaces.[19,41,42] We, therefore, reason that SFG, in combination with fluorescence microscopy, will reveal the surface structure of adsorbed proteins as a function of protein concentration on various surfaces.

In this study, we have investigated the effects of surface protein concentration, substrate hydrophobicity, and the nature of proteins on the spatial orientation of amino acids in adsorbed proteins using infrared−visible SFG vibration spectroscopy and fluorescence microscopy. We have chosen lysozyme, fibrinogen, and bovine serum albumin (BSA) as model proteins since their

adsorption behaviors, layer formations, and degrees of denaturation on various surfaces have been well characterized. Lysozyme is regarded as a hard protein because it resists denaturation and exhibits concentration-dependent layer formation. Soft proteins like BSA, however, undergo denaturation relatively easily upon adsorption.[12−16] Fibrinogen is a larger molecule with high surface affinity, which usually displaces preadsorbed proteins.[11,43] In this paper, SFG results are presented for the orientation and ordering of some amino acid residues in protein molecules adsorbed on hydrophilic silica and hydrophobic polystyrene surfaces as a function of surface concentration.

Experimental Section

SFG. The theory and experimental setup of SFG have been described in detail elsewhere.[44,45] Briefly, infrared−visible SFG vibrational spectroscopy involves a second-order nonlinear optical process in which two input beams, with frequencies ω_{ir} and ω_{vis}, overlap in a medium to generate an output at the sum frequency, ω_{sfg}. As a second-order nonlinear optical process, SFG is forbidden in media that possess inversion symmetry but allowed at surfaces and interfaces where inversion symmetry is broken. The intensity of the SFG signal, I_{sfg}, is proportional to the square of the surface nonlinear susceptibility:

$$I_{\mathrm{SFG}} \propto |\chi_{\mathrm{NR}}^{(2)} + \chi_{\mathrm{R}}^{(2)}|^2 = |\chi_{\mathrm{NR}}^{(2)} + \sum_q \frac{A_q}{\omega_{\mathrm{IR}} - \omega_q + i\Gamma}|^2 \quad (1)$$

with

$$A_{q,ijk} = n\sum_{lmn} a_{q,lmn}\langle(\hat{i}\cdot\hat{l})(\hat{j}\cdot\hat{m})(\hat{k}\cdot\hat{n})\rangle \quad (2)$$

$$a_{q,lmn} = -\frac{1}{2\epsilon_0\omega_q}\frac{\partial\mu_n}{\partial Q_q}\frac{\partial\alpha_{lm}}{\partial Q_q} \quad (3)$$

where $\chi_{\mathrm{NR}}^{(2)}$, $\chi_{\mathrm{R}}^{(2)}$, A_q, ω_q, Γ, $\langle\rangle$, μ_n, and α_{lm} are the nonresonant contribution, resonant contribution, oscillator strength, resonant frequency, width, average over orientation distribution, infrared dipole, and Raman tensor, respectively. The oscillator strength (A_q) is related to the number density of contributing oscillators (n), an orientation averaged coordinate transformation, and the product of derivatives of both the polarizability and dipole as shown in eqs 2 and 3 ($a_{q,lmn}$). Therefore, the vibrational mode must be both infrared and Raman active for a sum frequency signal to be resonantly enhanced. SFG spectra were collected with the $s_{\mathrm{sfg}}s_{\mathrm{vis}}p_{\mathrm{ir}}$ polarization combination (*ssp*), which specifically probes the *yyz* component of A_q, a 27-component tensor. Additional spectra were collected with the $s_{\mathrm{sfg}}p_{\mathrm{vis}}s_{\mathrm{ir}}$ polarization combination (*sps*), which is sensitive to the *yzy* component of A_q.

Laser System and Data Collection. SFG spectra were obtained with a passive−active mode-locked Nd:YAG laser (Leopard, Continuum, Santa Clara, CA). The 1064 nm light generated has a pulse width of ca. 20 ps and the laser operates at a 20 Hz repetition rate. Radiation is sent to an optical parametric generator/amplifier (OPG/OPA) stage (LaserVision, Bellevue, WA) where tunable infrared radiation is produced in addition to frequency-doubled radiation at 532 nm. The OPG/OPA consists of two parts. The first is an angle-tuned potassium titanyl phosphate (KTP) stage pumped with 532 nm light to generate near-infrared radiation between 1.35 and 1.85 μm. This output is then mixed with the 1064 nm fundamental in an angle-tunable potassium titanyl arsenate (KTA) stage to produce a tunable infrared beam from 2000 to 4000 cm^{-1} (7 cm^{-1} fwhm). The tunable infrared

(24) Norde, W. *Cell Mater.* **1995**, *5*, 97−112.
(25) Du, Q.; Freysz, E.; Shen, Y. R. *Phys. Rev. Lett.* **1994**, *72*, 238−241.
(26) Kim, J.; Cremer, P. S. *J. Am. Chem. Soc.* **2000**, *122*, 12371−12372.
(27) Kim, J.; Kim, G.; Cremer, P. S. *J. Am. Chem. Soc.* **2002**, *124*, 8751−8756.
(28) Baldelli, S.; Mailhot, G.; Ross, P.; Somorjai, G. A. *J. Am. Chem. Soc.* **2001**, *123*, 7697−7702.
(29) Chen, Z.; Ward, R.; Tian, Y.; Baldelli, S.; Opdahl, A.; Shen, Y. R.; Somorjai, G. A. *J. Am. Chem. Soc.* **2000**, *122*, 10615−10620.
(30) Gracias, D. H.; Chen, Z.; Shen, Y. R.; Somorjai, G. A. *Acc. Chem. Res.* **1999**, *32*, 930−940.
(31) Opdahl, A.; Phillips, R. A.; Somorjai, G. A. *J. Phys. Chem. B* **2002**, *106*, 5212−5220.
(32) Wang, J.; Chen, C.; Buck, S. M.; Chen, Z. *J. Phys. Chem. B* **2001**, *105*, 12118−12125.
(33) Wang, J.; Paszti, Z.; Even, M. A.; Chen, Z. *J. Am. Chem. Soc.* **2002**, *124*, 7016−7023.
(34) Wang, J.; Buck, S. M.; Even, M. A.; Chen, Z. *J. Am. Chem. Soc.* **2002**, *124*, 13302−13305.
(35) Wang, J.; Buck, S. M.; Chen, Z. *J. Phys. Chem. B* **2002**, *106*, 11666−11672.
(36) Gragson, D. E.; McCarty, B. M.; Richmond, G. L. *J. Am. Chem. Soc* **1997**, *119*, 6144−6152.
(37) Gragson, D. E.; Richmond, G. L. *J. Phys. Chem. B* **1998**, *102*, 3847−3861.
(38) Himmelhaus, M.; Eisert, F.; Buck, M.; Grunze, M. *J. Phys. Chem. B* **2000**, *104*, 576−584.
(39) Liu, Y.; Messmer, M. C. *J. Am. Chem. Soc.* **2002**, *124*, 9714−9715.
(40) Liu, Y.; Messmer, M. C. *Langmuir* **2001**, *17*, 4329−4335.
(41) Wertz, C. F.; Santore, M. M. *Langmuir* **1999**, *15*, 8884−8894.
(42) Mao, H.; Yang, T.; Cremer, P. S. *J. Am. Chem. Soc.* **2002**, *124*, 4432−4435.

(43) Schaaf, P.; Déjardin, P.; Schmitt, A. *Langmuir* **1987**, *3*, 1131−1135.
(44) Shen, Y. R. *Nature* **1989**, *337*, 519−525.
(45) Shen, Y. R. *Surf. Sci.* **1994**, *299/300*, 551−562.

Table 1. Representative Physical Properties of Model Proteins

protein	mass (Da)	size (nm)	p*I*	layer formation properties	refs
lysozyme	14 000	4 × 3 × 3	11.1	monolayer, multilayer[a]	*15, 16, 47*
fibrinogen	340 000	47 × 5 × 5	5.5	monolayer	*43, 46*
BSA	69 000	7 × 4 × 4	4.8	monolayer	*56, 63*

[a] Lysozyme is known to form a monolayer at low surface concentration, but multilayers are observed when the bulk concentration is high (see refs 15 and 16).

beam is combined with the 532 nm radiation at the sample interface at incident angles of ca. 50° and 40°, respectively, with respect to the surface normal. The SFG signal generated from the sample is collected by a photomultiplier tube, sent to a gated integrator, and stored digitally. For each scan, data is collected with 200 shots/data point in 5 cm^{-1} increments in the 2800−3100 cm^{-1} range and normalized by SFG intensity from a Z-cut quartz crystal measured at the sample stage. Although NH, OH, and amide bonds are of great significance for the identification of adsorbed proteins, our primary experiments focused on the CH stretch region, since adsorbed proteins are more likely to be covered with hydrocarbon-rich amino acids. In addition, obtaining strong infrared intensity in the amide bond stretch range is not possible due to present instrumental limitations. For a given condition, SFG measurements were repeated many times to increase the signal-to-noise ratio (at least three and five times for *ssp* and *sps* polarization combinations, respectively) and data were averaged to produce the final spectra presented in this paper.

Sample Preparation and Fluorescence Microscopy. The water used in the preparation of protein solutions and in the cleaning of the experimental apparatus was produced by a Millipore water purification system with a minimal resistivity of 18.0 MΩ·cm. BSA (99%, Sigma−Aldrich) was used as received, but fibrinogen (type IV, 95% clottable, Sigma−Aldrich) and lysozyme (95%, Sigma−Aldrich) were purified by size-exclusion chromatography on Sephadex G-100 and G-25 columns (Sigma−Aldrich), respectively, before use. The concentrations of purified proteins were determined by absorption measurements at 280 nm on a UV−visible spectrometer (Shimadzu UV-2100) with extinction coefficients of 2.64 and 1.51 mL/(cm·mg) for lysozyme and fibrinogen, respectively.[46,47] For all proteins, solutions at concentrations of 1.0, 0.2, 0.04, and 0.008 mg/mL were prepared with the use of 32 mM phosphate-buffered saline (PBS) at pH 7.0. Representative physical properties of these proteins are listed in Table 1.

Silica disks (diameter 0.5 in., thickness ¼ in., Esco Products) were cleaned in hot chromic acid for several hours, rinsed with copious quantities of purified water, and dried at room temperature before use. Clean silica surfaces are generally regarded as hydrophilic, since surfaces are terminated by titratable silanol groups (Si−OH).[48] A hydrophobic polystyrene thin film surface was prepared by spin-casting the polymer in toluene (3.0 wt %) at 3000 rpm onto a clean silica surface. Partially deuterated polystyrene (PS-d_3, MW ∼249 600, Polymer Source, Inc.) and perdeuterated polystyrene (PS-d_8, MW ∼372 000, Polymer Source, Inc.) were used in order to separate the contributions to the SFG signal from the adsorbed proteins and underlying polystyrene (see Figure 1 for structures). After casting, the films were annealed at 70 °C for 12 h. Ellipsometry measurements showed the thickness of the films to be about 300 nm.

Protein adsorption on both hydrophilic silica and hydrophobic polystyrene surfaces was carried out in bulk protein solutions with different concentrations for 5 days to allow complete denaturation. Solid substrates with adsorbed proteins were rinsed to remove loosely coagulated proteins by use of protein-free PBS. Samples were stored

(46) *Human Protein Data*; Haeberli, A., Ed.; WILEY−VCH: Weinheim, 1998.
(47) *Lysozyme*; Osserman, E. F.; Canfield, R. E.; Beychok, S., Eds.; Academic Press: New York, 1974.
(48) Iler, R. K. *The Chemistry of Silica*; Wiley: New York, 1979.
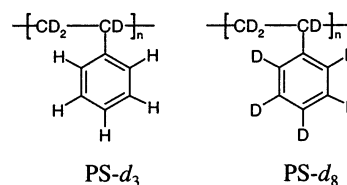
Figure 1. Structures of partially deuterated polystyrene (PS-d_3) and perdeuterated polystyrene (PS-d_8).

separately in protein-free PBS just before data collection. During the data collection, samples are located in a closed container with saturated vapor to prevent adsorbed proteins from dehydrating.

Fluorescence measurements to determine the concentrations of proteins adsorbed on surfaces were carried out on a Nikon Diaphot 200 inverted microscope using a 10× phase 1 DL objective. Fluorescence images were taken with the same objective in fluorescence mode with a 100 W mercury arc lamp. Images were recorded with a digital color CCD camera (Diagnostic Instruments model 1.3.0) that was driven by the manufacturer's spot image collection software. Texas Red-conjugated BSA (Molecular Probes), Alexa Fluor 594-conjugated fibrinogen (Molecular Probe), and tetramethylrhodamine isothiocyanate-(TRITC-) conjugated lysozyme were used to prepare protein solutions at concentrations of 1.0, 0.2, 0.04, and 0.008 mg/mL.

Labeling of TRITC on lysozyme was carried out by use of tetramethylrhodamine 5-isothiocyanate (5-TRITC, G isomer, Molecular Probes), as described elsewhere.[19,49] Briefly, ca. 15 mL of lysozyme solution at a concentration of 20 mg/mL was prepared in a 0.2 M sodium bicarbonate (Sigma−Aldrich) solution. 5-TRITC (5 mg) dissolved in 0.5 mL of DMSO was slowly added to the lysozyme solution with stirring. The reaction was allowed to proceed for 2 h and then stopped by adding 0.1 mL of 1.5 M hydroxylamine (Sigma−Aldrich). The solution was stirred for another hour. Finally, TRITC-labeled lysozyme was separated on a Sephadex G-25 column (Sigma−Aldrich) and the concentration was determined by adsorption measurements at 280 nm on a UV−visible spectrometer (Shimadzu UV-2100). The dye-to-protein ratio was ca. 1.3, which is in good agreement with previous data.[19] In this work, fluorophore-labeled proteins were used to determine the surface concentration, while SFG experiments were carried out with unlabeled proteins. Both labeled and unlabeled proteins were absorbed on surfaces under the same experimental conditions to achieve identical surface concentrations and structures.

Results

(a) Determination of the Relative Surface Protein Concentration by Fluorescence Microscopy. The relative amounts of protein adsorbed on hydrophobic polystyrene and hydrophilic silica surfaces were determined by fluorescence measurements.[11,19,50] As the labeled protein molecules contain a nearly identical number of conjugated fluorophores and their quantum yields are nearly constant regardless of the protein conformation, measured fluorescence intensities are proportional to the amount of adsorbed protein for a given area.[11,19,50] The results are presented in Figure 2. For lysozyme, the relative amounts adsorbed on both hydrophilic and hydrophobic surfaces increase in proportion to the bulk protein concentration (Figure 2a). Similarly, more fibrinogen and BSA molecules are present on both hydrophilic and hydrophobic surfaces when adsorption is carried out at higher bulk protein concentrations (Figure 2b,c).
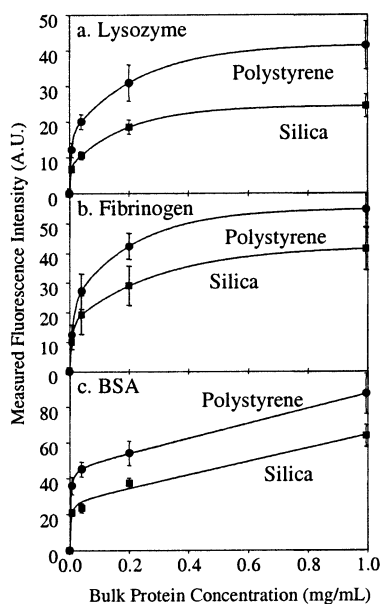
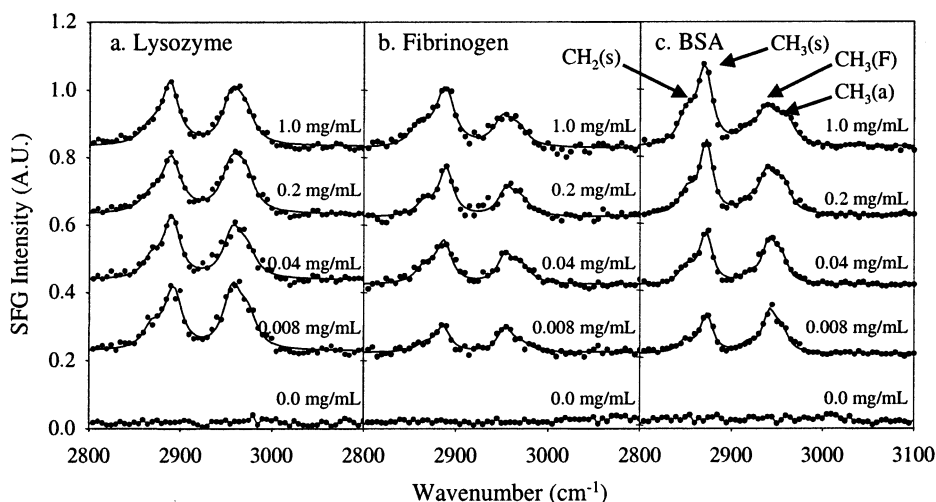(49) Brinkley, M. *Bioconjugate Chem.* **1992**, *3*, 2−13.
(50) Horsley, D.; Herron, J.; Hlady, V.; Andrade, J. D. In *Proteins at Interfaces: Physicochemical and Biochemical Studies*; American Chemical Society: Washington, DC, 1987; pp 290−305.

Figure 2. Relative amounts of protein adsorbed on hydrophilic silica and hydrophobic polystyrene surfaces as a function of bulk concentration for (a) lysozyme, (b) fibrinogen, and (c) BSA. These results are obtained by measuring the fluorescence intensity of tetramethylrhodamine isothiocyanate- (TRITC-) conjugated lysozyme, Alexa Fluor 594-conjugated fibrinogen, and Texas Red-conjugated BSA by fluorescence microscopy. Note that more protein molecules adsorb on hydrophobic surfaces than on hydrophilic substrates at a corresponding bulk protein concentration. Solid lines denote fitted data.

It was also found that hydrophobic polystyrene surfaces immobilize more proteins than do hydrophilic surfaces for a given bulk protein concentration over the concentration range investigated (ca. 1.5, 1.8, and 1.5 times more for lysozyme, fibrinogen, and BSA, respectively). This result is in good agreement with previous reports.[12,17,50−52]

(b) SFG Studies of Adsorbed Proteins on Hydrophilic Silica Surfaces. Figure 3 shows SFG spectra in the CH stretch region for lysozyme, fibrinogen, and BSA adsorbed on hydrophilic silica surfaces from solutions with different bulk protein concentrations (1.0, 0.2, 0.04, 0.008, and 0.0 mg/mL). The

Table 2. Oscillator Strengths for $CH_3(s)$ and $CH_3(a)$ Modes Obtained from Fitting the Data in Figures 3 and 4 to Eq 1

proteins	bulk protein concn (mg/mL)	$A_{CH_3(s)}$ around 2875 cm^{-1}		$A_{CH_3(a)}$ around 2960 cm^{-1}	
		ssp	sps	ssp	sps
lysozyme	1.0	4.07 ± 0.19	0	1.96 ± 0.23	1.94 ± 0.21
	0.2	4.13 ± 0.18	0	1.75 ± 0.24	1.98 ± 0.20
	0.04	4.11 ± 0.21	0	2.03 ± 0.19	1.94 ± 0.22
	0.008	4.26 ± 0.20	0	1.90 ± 0.22	1.82 ± 0.23
fibrinogen	1.0	4.59 ± 0.19	0	1.54 ± 0.24	2.15 ± 0.19
	0.2	3.54 ± 0.21	0	1.75 ± 0.26	1.95 ± 0.21
	0.04	3.05 ± 0.24	0	1.68 ± 0.25	1.55 ± 0.24
	0.008	2.31 ± 0.27	0	1.54 ± 0.25	1.50 ± 0.24
BSA	1.0	5.00 ± 0.21	0	2.19 ± 0.19	2.00 ± 0.24
	0.2	4.20 ± 0.19	0	2.03 ± 0.22	1.71 ± 0.25
	0.04	3.72 ± 0.16	0	2.03 ± 0.21	1.32 ± 0.24
	0.08	3.11 ± 0.20	0	2.00 ± 0.23	1.11 ± 0.27

polarization combination used was *ssp*, with respect to SFG signal, visible input, and infrared input components, respectively. The solid lines represent least-squares fits of the raw data to eq 1 to obtain oscillator strengths (A_q), peak positions, and widths. Some representative fitting parameters are listed in Table 2. The fitted SFG spectra show that there are four vibrational modes around 2853, 2875, 2940, and 2960 cm^{-1}. They are assigned to the CH_2 symmetric stretch [$CH_2(s)$], CH_3 symmetric stretch [$CH_3(s)$], CH_3 Fermi resonance [$CH_3(F)$], and CH_3 asymmetric stretch [$CH_3(a)$] modes, respectively.[35−38]

Several features are observed in the SFG spectra. Although the amounts of lysozyme adsorbed on silica surfaces significantly vary depending on the bulk protein concentration, the SFG spectra do not show considerable differences (Figure 3a). In contrast, fibrinogen and BSA molecules adsorbed on silica surfaces exhibit concentration-dependent SFG signal intensities and peak shapes (Figure 3b,c). In Figure 3b, the SFG signal intensity of the $CH_3(s)$ mode at 2875 cm^{-1} proportionally increases with the number of fibrinogen molecules adsorbed on hydrophilic surfaces, while the $CH_3(F)$ and $CH_3(a)$ modes around 2940 and 2960 cm^{-1} exhibit nearly constant signal intensity, regardless of the adsorption conditions. A similar trend is also observed in the SFG spectra for BSA adsorbed on hydrophilic silica surfaces (Figure 3c). Differences in the
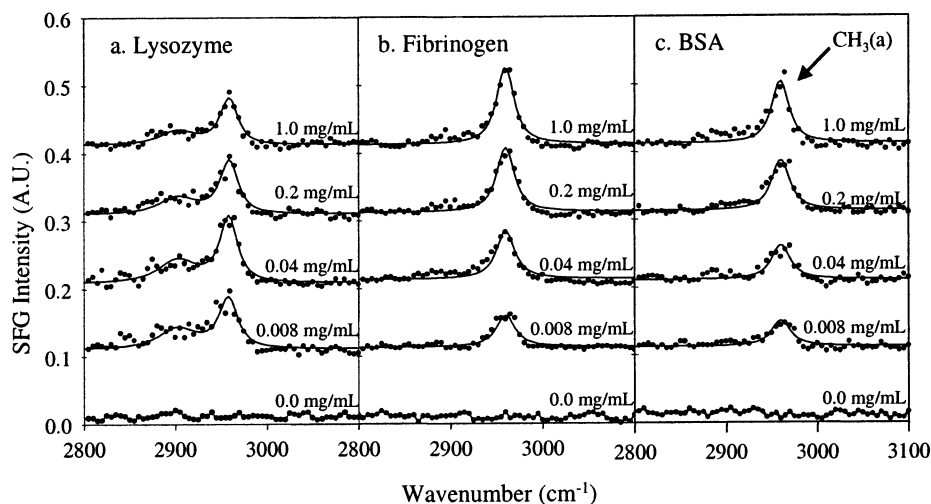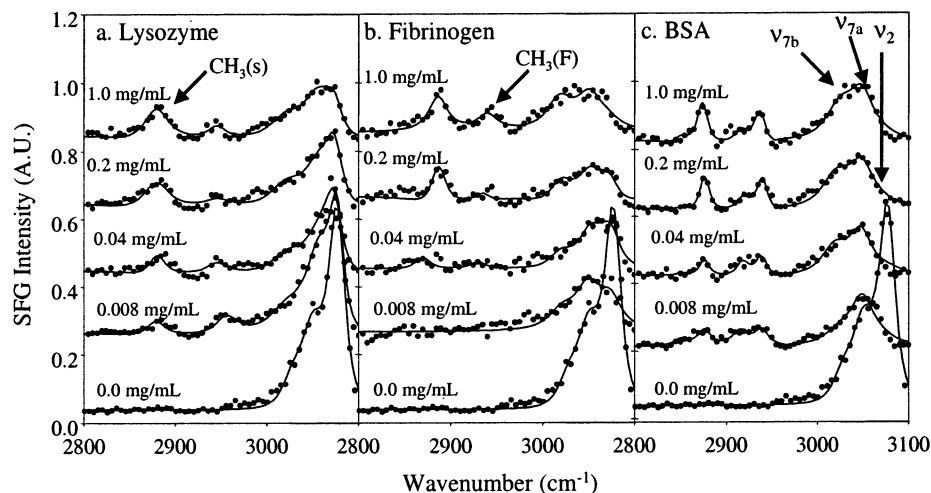

Figure 3. SFG spectra of (a) lysozyme, (b) fibrinogen, and (c) BSA adsorbed on hydrophilic silica surfaces. Deposition of proteins is carried out in bulk protein solutions with concentrations of 1.0, 0.2, 0.04, 0.008, and 0.0 mg/mL. Filled circles denote collected data and the solid lines are data fit to eq 1, from which peak positions, widths, and oscillator strengths can be obtained. The beam polarization combinations are *s* (sum frequency), *s* (visible), and *p* (infrared), respectively. Note that the SFG signal intensity is independent of the lysozyme bulk concentration but changes with solution concentration for fibrinogen and BSA.

Figure 4. SFG spectra of (a) lysozyme, (b) fibrinogen, and (c) BSA adsorbed on hydrophilic silica surfaces deposited from bulk protein solutions with concentrations of 1.0, 0.2, 0.04, and 0.008 mg/mL. Filled circles denote collected data and the solid lines are data fit to eq 1. The beam polarization combinations are *s* (sum frequency), *p* (visible), and *s* (infrared), respectively. The SFG signal intensity was multiplied by 4.


Figure 5. SFG spectra of (a) lysozyme, (b) fibrinogen, and (c) BSA adsorbed on hydrophobic polystyrene (PS-d_3) surfaces. The protein deposition is carried out in bulk solutions with concentrations of 1.0, 0.2, 0.04, 0.008, and 0.0 mg/mL. The beam polarization combinations are *s* (sum frequency), *s* (visible), and *p* (infrared), respectively. Note that while more protein molecules adsorb on hydrophobic surfaces than on hydrophilic surfaces, the SFG signal intensities are lower.

concentration-dependent SFG spectra for adsorbed proteins are attributed to differences in the orientation and ordering of the amino acid residues in these proteins at the surface.

To obtain additional information for the orientation and ordering of methyl groups in adsorbed proteins, SFG experiments were conducted with the *sps* polarization combination and the results are shown in Figure 4. Curve-fitting parameters for the SFG spectra in Figure 4 are listed in Table 2. All SFG spectra contain feature around 2960 cm^{-1}, corresponding to the CH$_3$(a) mode, but do not contain the CH$_3$(s) mode, which normally appears around 2875 cm^{-1}. Some spectra, particularly those in Figure 4a, contain a broad SFG peak between 2890 and 2920 cm^{-1}, but it is uncertain which vibrational mode(s) are responsible for the observed signal intensity. In Figure 4a, the intensities of the CH$_3$(a) mode for lysozyme on hydrophilic silica surfaces are nearly comparable, regardless of the surface concentration. Fibrinogen and BSA molecules adsorbed on silica surfaces, however, exhibit concentration-dependent SFG signal intensities (Figure 4b,c). The SFG signal intensity of the CH$_3$-

(a) mode at 2960 cm^{-1} increases with the number of fibrinogen and BSA molecules adsorbed on hydrophilic surfaces.

(c) SFG Studies of Adsorbed Proteins on Hydrophobic Polystyrene Surfaces. Figure 5 shows SFG spectra collected from proteins adsorbed on hydrophobic polystyrene (PS-d_3, see Figure 1) surfaces using the same bulk protein solutions with identical adsorption times. SFG spectra contain several features for the CH stretch modes in the 2800 and 3000 cm^{-1} range, but the CH$_3$(a) mode at 2960 cm^{-1} is no longer observed. In Figure 5a, the SFG intensities of these features generally increase in proportion to the surface lysozyme concentration. This is opposite to that observed for hydrophilic surfaces, where the SFG signal intensity is nearly independent of the lysozyme concentration (see Figure 3a). The SFG spectra for fibrinogen and BSA on hydrophobic surfaces are somewhat similar compared to those for lysozyme except for the fact that fibrinogen molecules adsorbed at lower bulk concentrations (0.04 and 0.008 mg/mL) do not exhibit an observable SFG signal intensity (Figure 5b). In general, the SFG signal for adsorbed

ν_{7b} (3027 cm^{-1}) ν_{7a} (3053 cm^{-1}) ν_2 (3073 cm^{-1})
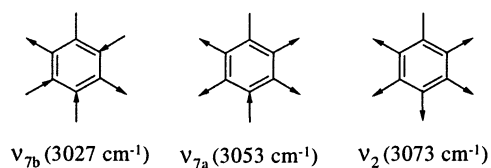
Figure 6. Vibrational normal modes for phenyl rings in polystyrene.

proteins on hydrophobic surfaces exhibits less intensity than that for hydrophilic surfaces at a given adsorption condition, despite more protein molecules present on hydrophobic surfaces. Again, we propose that the differences in the SFG signal intensity for proteins between hydrophilic and hydrophobic surfaces are due to the structural differences in adsorbed proteins on surfaces.

In addition, the SFG spectra in Figure 5 contain several features in the 3000−3100 cm^{-1} range that are responsible for the CH stretch modes of the phenyl ring in the underlying polystyrene. This is confirmed by experiments with perdeuterated polystyrene (PS-d_8, see Figure 1 for structure) that does not contain CH bonds. Without adsorbed proteins, a large peak at 3073 cm^{-1} and a shoulder around 3053 cm^{-1} are observed. They are responsible for the ν_2 and ν_{7a} modes, respectively (see Figure 6).[53,54] It was found that the SFG intensity of the ν_2 mode slowly attenuates, as more lysozyme molecules are present. Fibrinogen adsorption yielded similar effects on the intensity of the ν_2 mode. However, the SFG intensity of the ν_2 mode is more rapidly suppressed and a new mode around 3027 cm^{-1} appears, as more fibrinogen molecules are present. In both cases, the intensity of the ν_2 mode is less affected, compared to the case of BSA adsorption, where even a small amount of BSA deposition completely suppresses the intensity of the ν_2 mode (Figure 5c). The results indicate that the structure and orientation of the underlying phenyl ring in the polystyrene substrate is affected by protein deposition, presumably due to the interaction between phenyl rings and adsorbed protein molecules.

Although we attempted to obtain SFG data with the *sps* polarization combination, the signal-to-noise ratio was too low to extract any reliable structural information. This is presumably due to the random and isotropic orientation of methyl groups in adsorbed proteins as shown in the SFG data collected under the *ssp* polarization combination shown in Figure 5.

Discussion

In Figures 3−5, the SFG signal intensity for the CH stretch modes in the 2800−3000 cm^{-1} range varies with protein concentration, surface hydrophobicity, and the nature of proteins adsorbed. This indicates that the spatial orientation and ordering of amino acids in adsorbed proteins are significantly affected by the adsorption conditions via different denaturation and layer formation behaviors after proteins are initially adsorbed on solid substrates. The SFG signal intensity, I_{sfg}, is governed by the surface number density and orientation average of the hyperpolarizability for a given vibrational mode. Thus, we propose that the SFG data and relative surface concentrations obtained

from fluorescence microscopy may provide structural information regarding amino acid residues containing methyl groups in adsorbed proteins.[55] At present, however, we cannot identify the amino acids that are responsible for the SFG signal intensity since all proteins contain a number of amino acid residues with methyl groups.[46,47,56]

It is well-known that the extent of denaturation primarily depends on the surface coverage of the adsorbed protein.[1,2,12,13] If there are less protein molecules on the surface, they are more likely to spread out until the process is prevented by neighboring proteins. Conversely, less structural rearrangement is allowed if more proteins are deposited on the surface from solutions with higher bulk protein concentrations. The other important factor for denaturation is the surface hydrophobicity.[13,14,57,58] Adsorbed proteins undergo significant structural rearrangement if interactions between proteins and surfaces are strong enough to overcome the internal structure of proteins sustained by disulfide bonds and hydrogen bonding.[1,2] In addition, the nature of proteins is also known to affect the denaturation process. While soft proteins like BSA undergo significant denaturation by losing α-helix content upon adsorption on silica surfaces, hard proteins like lysozyme tend to resist denaturation under the same experimental conditions.[12,13]

(a) Proteins on Hydrophilic Silica Surfaces. For quantitative analysis, we obtained the oscillator strengths of the CH$_3$(s) and CH$_3$(a) modes, $A_{CH_3(s)}$ and $A_{CH_3(a)}$, from the SFG spectra of proteins adsorbed on hydrophilic surfaces in Figure 3 (see Table 2). The magnitude of the oscillator strength ratio, $A_{CH_3(s)}/A_{CH_3(a)}$, contains information regarding the relative orientation of methyl groups in adsorbed proteins.[31,59] Simply, as the $A_{CH_3(s)}/A_{CH_3(a)}$ ratio increases, amino acids containing methyl groups tilt less with respect to the surface normal. Figure 7a shows the $A_{CH_3(s)}/A_{CH_3(a)}$ ratio plotted as a function of relative surface protein concentration[55] for lysozyme, fibrinogen, and BSA.

For lysozyme, the $A_{CH_3(s)}/A_{CH_3(a)}$ ratio is nearly constant regardless of the surface concentration. The results suggest that the spatial orientation of methyl groups in adsorbed lysozyme is not affected by the surface number density. Other structural information can be obtained from the concentration-independent magnitude of the oscillator strength of the CH$_3$(s) mode [$A_{CH_3(s)}$] shown in Figure 7b. This implies that the number density of SFG-active methyl groups is comparable, although a different number of lysozyme molecules are present on the surface. On the contrary, the $A_{CH_3(s)}/A_{CH_3(a)}$ ratios for fibrinogen and BSA increase with surface number density, indicating that SFG-active methyl groups in fibrinogen and BSA become less tilted with respect to the surface normal as more protein molecules are present on the surface. Furthermore, the magnitude of $A_{CH_3(s)}$ increases proportionally with the surface protein density (see Figure 7b).

We attempted to obtain more quantitative structural information on the average orientation of methyl groups in adsorbed

(51) Chen, J.; Dong, D. E.; Andrade, J. D. *J. Colloid Interface Sci.* **1982**, *89*, 577−580.
(52) Norde, W.; Lyklema, J. *J. Colloid Interface Sci.* **1978**, *66*, 257−265.
(53) Gautam, K. S.; Schwab, A. D.; Dhinojwala, A. *Phys. Rev. Lett.* **2000**, *85*, 3854−3857.
(54) Zhang, D.; Dougal, S. M.; Yeganeh, M. S. *Langmuir* **2000**, *16*, 4528−4532.
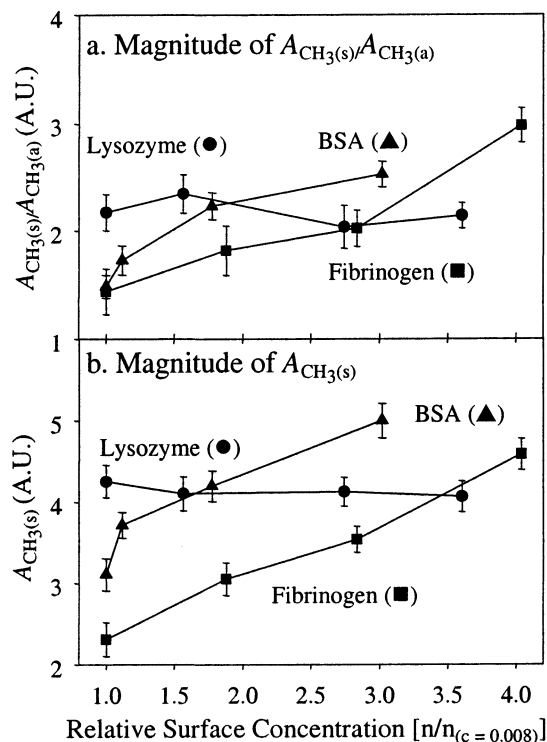
(55) The relative surface concentration is defined as the ratio of fluorescence intensity for adsorbed proteins at a given bulk concentration normalized to that obtained in solution with a concentration of 0.008 mg/mL.
(56) Peters, T. J. *All about Albumin Biochemistry, Genetics, and Medical Applications*; Academic Press: San Diego, 1996.
(57) Norde, W.; Zoungrana, T. *Biotechnol. Appl. Biochem.* **1998**, *28*, 133−143.
(58) Yan, G.; Li, J.-T.; Huang, S.-C.; Caldwell, K. D. In *Proteins at Interfaces II: Fundamentals and Applications*; Horbett, T. A., Brash, J. l., Eds.; American Chemical Society: Washington, DC, 1995; pp 256−268.
(59) Hirose, C.; Yamamoto, H.; Akamatsu, N.; Domen, K. *J. Phys. Chem.* **1993**, *97*, 10064−10069.

Figure 7. (a) Ratios of the oscillator strengths of the CH$_3$(s) and CH$_3$(a) modes, $A_{CH_3(s)}/A_{CH_3(a)}$, and (b) oscillator strength magnitude of the CH$_3$(s) mode, $A_{CH_3(s)}$, for lysozyme (●), fibrinogen (■), and BSA (▲) as a function of the relative surface concentration of proteins adsorbed on hydrophilic silica surfaces.[55]
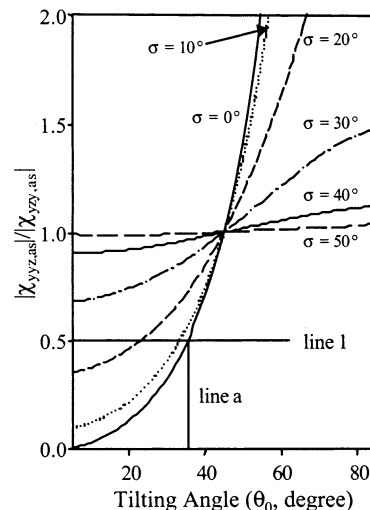

Figure 8. Calculated $|\chi_{yyz,as}|/|\chi_{yzy,as}|$ ratio for the methyl group in adsorbed proteins as a function of tilting angle, θ_0, and angle distribution, σ.

proteins at the interface by analyzing the SFG spectra obtained under the s*sp* and *sps* polarization combinations (Figures 3 and 4). Details on calculating the orientation of molecules at surfaces can be found elsewhere.[32,33,60,61] In brief, for the CH$_3$(a) mode of a methyl group with C$_{3v}$ symmetry, it can be shown that

$$\left|\frac{\chi_{yyz,as}}{\chi_{yzy,as}}\right| = \left|\frac{\langle\cos\theta\rangle - \langle\cos^3\theta\rangle}{\langle\cos^3\theta\rangle}\right| \tag{4}$$

$$\langle\cos^n\theta\rangle = \int_{-1}^{1}\cos^n\theta\, f(\theta)\sin\theta\, d\theta \tag{5}$$

where *x*,*y*,*z* denotes the lab frame coordinates, with the *z* axis along the surface normal, *f*(θ) is the distribution function of the orientation angles, and θ is the angle between the molecular axis of the methyl group and the surface normal. The $|\chi_{yyz,as}|/|\chi_{yzy,as}|$ ratio can be obtained from fitting parameter A_q listed in Table 2. More realistically, surface methyl groups are expected to have a range of possible orientations. To account for this, the orientation distribution function, *f*(θ), is introduced as a Gaussian, $P(\theta) = \exp[-(\theta - \theta_0)^2/2\sigma^2]$, where σ is the distribution width for the tilting angle θ_0 with respect to the surface normal.

Figure 8 shows the calculated $|\chi_{yyz,as}|/|\chi_{yzy,as}|$ ratio of the methyl group as a function of tilting angle, θ_0, for several distribution widths (σ = 0°, 10°, 20°, 30°, 40°, and 50°). Figure 8 also indicates that there are many solutions for a given value of $|\chi_{yyz,as}|/|\chi_{yzy,as}|$. For example, if $|\chi_{yyz,as}|/|\chi_{yzy,as}|$ is 0.5, one of

the possible solutions occurs at $\theta_0 = 35°$ and $\sigma = 0°$ (a δ function; see lines 1 and a in Figure 8). Another possible solution is $\theta_0 = 0°$ and $\sigma = 24°$ (intersection of line 1 and *y*-axis in Figure 8). The latter solution implies a broad distribution for the tilting angle. The first solution implies that if we assume the methyl group orientation distribution is a δ function ($\sigma = 0°$), the tilting angle, θ_0, is found to be about 35°. Similarly, if we assume that all methyl groups are perpendicular to the surface ($\theta_0 = 0°$), the distribution of the tilting angle, σ, is found to be about 24°.

For methyl groups in adsorbed lysozyme, the fitting parameters in Table 2 yield a $|\chi_{yyz,as}|/|\chi_{yzy,as}|$ ratio in the range of 0.9–1.0, regardless of the surface concentration. From Figure 8, the tilting angle of methyl groups in adsorbed lysozyme is found to lie between 43° and 46° with respect to the surface normal for the case of a δ function distribution (σ = 0°). The $|\chi_{yyz,as}|/|\chi_{yzy,as}|$ ratio of fibrinogen, however, is more concentration-dependent. When it is adsorbed in the solution with a concentration of 0.008 mg/mL, the ratio is ca. 1.1, which corresponds to a tilting angle of 46° from the surface normal, with a δ function distribution. Methyl groups become less tilted when adsorbed at higher bulk concentrations. The $|\chi_{yyz,as}|/|\chi_{yzy,as}|$ ratio is about 0.7, producing a corresponding tilting angle of 40° from the surface normal for a δ function distribution. Methyl groups in adsorbed BSA show similar concentration-dependent tilting angle behavior, in which the $|\chi_{yyz,as}|/|\chi_{yzy,as}|$ ratio is in the range of 1.8–1.1 with equivalent tilting angles between 46° and 53° from the surface normal with a δ function distribution.

The concentration-dependent tilting angles for methyl groups in adsorbed lysozyme, fibrinogen, and BSA seem to be related to differences in the layer formation and denaturation properties of these proteins. Previous circular dichroism (CD) and X-ray reflectivity studies have shown that lysozyme exhibits a negligible degree of structural denaturation even when a small amount is present on silica surfaces.[12,13,15,16] X-ray reflectivity data have also revealed that lysozyme exhibits concentration-dependent layer formation properties on silica surfaces.[15,16] At lower bulk concentrations, lysozyme forms a monolayer with a thickness close to the length of the molecular axis of native lysozyme. When the bulk protein concentration is raised, a

(60) Zhuang, X.; Miranda, P. B.; Kim, D.; Shen, Y. R. *Phys. Rev. B* **1999**, *59*, 12632–12640.
(61) Hirose, C.; Akamatsu, N.; Domen, K. *Appl. Spectrosc.* **1992**, *46*, 1051–1072.
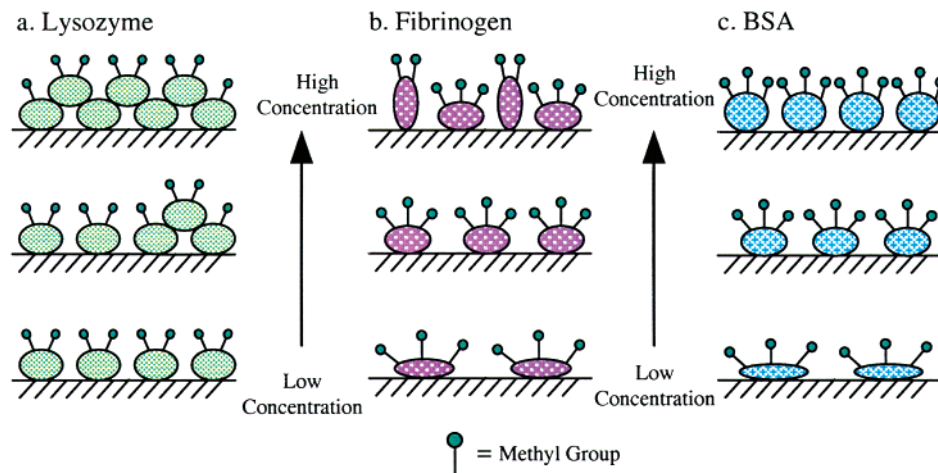
Figure 9. Proposed model for the orientation of methyl groups in (a) lysozyme, (b) fibrinogen, and (c) BSA adsorbed on hydrophilic silica surfaces with different surface concentrations. Although proteins are hydrated, water molecules are omitted for clarity. The dimensions of the adsorbed proteins in each figure are not the same. It is difficult to describe the adsorption of protein molecules on hydrophobic polystyrene surfaces by a simple model.

multilayer with a similar footprint is formed with corresponding enhancements in the layer thickness. Therefore, we can expect that SFG-active methyl groups on the surface have a similar number density with a relatively identical orientation due to the negligible degree of denaturation and layer formation properties on surfaces, regardless of the bulk concentration. Figure 9a illustrates the molecular packing and orientation of methyl groups of lysozyme molecules on silica surfaces with different surface concentrations. This model explains the concentration-independent SFG signal intensity for the CH$_3$(s) mode in Figures 3a and 4a.

Fibrinogen molecules exhibit different adsorption properties on silica surfaces in terms of denaturation and layer formation. CD data have shown that the α-helix content of fibrinogen adsorbed on hydrophilic surfaces decreases somewhat.[62] Ellipsometry measurements have revealed that the layer formation by fibrinogen is affected by the bulk protein concentration.[43] By comparing molecular dimensions and surface coverages, fibrinogen has been proposed to form a monolayer with its long axis parallel to the surface when the bulk protein concentration is low. The layer becomes thinner by spreading if the adsorption is conducted at even lower concentrations. Upon raising the surface coverage, some fibrinogen molecules begin to adopt a conformation with their long axes perpendicular to the surface, giving rise to the corresponding layer thickness, as illustrated in Figure 9b. According to this model, SFG-active methyl groups on surfaces have a different number density and orientation depending on the surface concentration. As more fibrinogen molecules are present on the surface, we assume that methyl groups tilt less with respect to the surface normal, as indicated by the concentration-dependent SFG spectra shown in Figures 3b and 4b.

Unlike these two proteins, BSA easily undergoes denaturation on hydrophilic silica surfaces.[12,13] It was observed that the α-helix content of BSA was reduced by ca. 50% after adsorption on hydrophilic silica surfaces by CD spectroscopy.[12] In addition, BSA exhibits different layer formation properties compared to those for lysozyme and fibrinogen. Ellipsometry measurements

have revealed that BSA forms a monolayer with a thickness always less than 40 Å on silica, indicating that adsorption is carried out with its long axis parallel to the surface.[63] The increase in the layer thickness with bulk protein concentration suggests that the extent of denaturation is reduced as the surface concentration increases. Thus, we suppose that the spatial orientation and ordering of amino acids depends on the surface concentration, as illustrated in Figure 9c. A more compact packing of BSA molecules on the surface causes methyl groups to tilt less with respect to the surface normal, as in the case of fibrinogen. This might be responsible for the concentration-dependent SFG spectra presented in Figures 3c and 4c.

(b) Proteins on Hydrophobic Polystyrene Surfaces. The SFG spectra for lysozyme, fibrinogen, and BSA adsorbed on hydrophobic surfaces in Figure 5 exhibit different features compared to those obtained from hydrophilic surfaces shown in Figure 3. Since the CH$_3$(a) mode at 2960 cm^{-1} is not observed, the ratio of the oscillator strengths of the CH$_3$(s) and CH$_3$(a) modes [$A_{CH_3(s)}/A_{CH_3(a)}$] in the SFG spectra of both surfaces cannot be compared. However, curve-fitting results reveal that the magnitude of all CH stretch modes is generally proportional to the relative surface concentration. Moreover, the SFG signal intensity for these modes is much weaker compared to the corresponding hydrophilic surface, despite the higher surface protein concentration.

In general, protein adsorption on hydrophobic surfaces is considerably different from that on hydrophilic surfaces. The major difference is that hydrophobic interactions between proteins and surfaces are more likely to cause a significant breakdown in the secondary structure. In fact, neutron reflectivity and calorimetry studies have independently shown that lysozyme loses a considerable amount of secondary structure on hydrophobic surfaces, despite its structural stability on hydrophilic surfaces.[14,58] Fibrinogen and BSA are also known to lose a larger amount of α-helical structure on hydrophobic surfaces.[58,64] Therefore, we assume that the orientation of SFG-active methyl groups in these proteins is more randomly

(62) Yongli, C.; Xiufang, Z.; Yandao, G.; Nanmming, Z.; Tingying, Z.; Xinqi, S. *J. Colloid Interface Sci.* **1999**, *214*, 38−45.

(63) Su, T. J.; Lu, J. R.; Thomas, R. K.; Cui, Z. F.; Penfold, J. *J. Phys. Chem. B* **1998**, *102*, 8100−8108.

(64) Lu, D. R.; Park, K. *J. Colloid Interface Sci.* **1991**, *144*, 271−281.

distributed and less concentration-dependent. This might be responsible for the SFG spectra with less intensity on hydrophobic surface compared to the corresponding hydrophilic surfaces, despite a higher number density (see Figures 3 and 5). Therefore, the increase in the surface number density of methyl groups is responsible for the simultaneous enhancement in the SFG signal intensity for all CH_x ($x = 2$ and 3) stretch modes in Figure 5.

Protein adsorption affects the orientation and ordering of phenyl groups in the underlying polystyrene surface. In Figure 5, the SFG signal intensity at 3073 cm^{-1} attenuates when protein molecules are present on the surface. This peak is responsible for the totally symmetric stretch mode of the phenyl ring (ν_2, see Figure 6). As the phenyl ring in polystyrene tilts ca. 20° with respect to the surface normal,[53,54] our SFG results indicate that the ν_2 mode is partially blocked after protein deposition. Considering the reduction in the SFG signal intensity, BSA binds to polystyrene surfaces in such a way as to affect the ν_2 mode more significantly than do fibrinogen and lysozyme. Curve-fitting shows that the magnitude of the ν_{7a} mode is not affected by protein adsorption. Interestingly, the ν_{7b} mode around 3027 cm^{-1} appears with an increasing number of fibrinogen and BSA molecules on the surface.

These results show interesting trends. Although the relative amounts of proteins adsorbed on polystyrene surfaces cannot be compared from the same bulk concentration, the greatest reduction in the SFG signal intensity for the ν_2 mode was achieved by BSA adsorption, followed by fibrinogen and lysozyme. The results suggest that each protein molecule interacts with phenyl rings in a different way, giving rise to different changes in the orientation and ordering of the underlying phenyl ring. The adsorption behavior of fibrinogen, in terms of spreading on hydrophilic surfaces and interacting with phenyl rings, is somewhat similar to that of BSA but quite different from that observed for lysozyme.

Summary and Conclusions

We conducted SFG experiments for lysozyme, fibrinogen, and BSA adsorbed on hydrophilic and hydrophobic surfaces with different surface protein concentrations in order to correlate the macroscopic adsorption conditions with the spatial orientation of amino acid residues. Our SFG data shows that the orientation of methyl groups in adsorbed proteins is intimately affected by the degree of denaturation and the difference in the layer formation, which is governed by the surface concentration of adsorbed protein, the hydrophobicity of the solid substrate, and the nature of the protein used. On hydrophilic surfaces, lysozyme molecules yield nearly concentration-independent SFG spectra, whereas the signal intensity for fibrinogen and BSA increases with surface concentration. The results indicate that the orientation of methyl groups in adsorbed lysozyme is concentration-independent, but those in BSA and fibrinogen become less tilted with respect to the surface normal with increasing protein concentration. However, methyl groups in protein adsorbed on hydrophobic surfaces appear more randomly oriented and produce a weaker SFG signal, even though more protein molecules are deposited on the surface compared to on hydrophilic surfaces. In addition, SFG results reveal that the orientation and ordering of phenyl rings in hydrophobic polystyrene surfaces are affected by protein deposition.

JA028987N